

Photocurrent and Photoluminescence Investigations of GaInNAs and GaInNAs(Sb) Quantum Wells Grown by Molecular Beam Epitaxy

¹S. Ben Bouzid, ¹F. Bousbih, ¹A. Hamdouni, ¹R. Chtourou, ²J.C. Harmand and ²P. Voisin

¹Laboratoire de Photovoltaïque et des Semiconducteurs, Institut National de Recherche Scientifique et Technique, BP.95, Hammam-Lif 2050, Tunisia, Tunis

²Laboratoire de Photonique et de Nanostructures, CNRS, Route de Nozay, 91460 Marcoussis, France

Abstract: We have investigated photocurrent (PC) and photoluminescence (PL) in sequentially grown GaInNAs/GaAs and GaInNAs(Sb)/GaAsSbN quantum wells. Photocurrent transitions are analyzed by theoretical calculations using envelope function formalism taking into account the strain effect and the strong coupling between nitrogen localized state and the GaInAs band gap. The results are consistent with a type I band alignment and a conduction band offset ratio of about 80 %. Additionally, our results suggest an increase of the electron effective mass by as much as 0.035 m_0 resulting from the flattening of the conduction band under nitrogen effect. The temperature evolution of the PL peak energy and the integrated PL intensity of GaInNAsSb QW show evidence of strong localization of carriers. Both, the high delocalization temperature, in the 230 K range and the strong shift between the PC and PL spectra of GaInNAsSb QW, indicate the presence of deeper localized states as compared to that in the GaInNAs QW.

Key words: GaInNAs, GaInNAsSb, photocurrent, photoluminescence, molecular beam epitaxy

INTRODUCTION

Proposed by Kodow et al.^[1], InGaAsN opens up new opportunities to realize low-cost, high performance 1.3 μm emitting semiconductor diode lasers grown on GaAs substrates. With intensive research effort, high performance 1.3 μm emitting InGaAsN quantum well (QW) lasers have been successfully reported using both molecular beam epitaxy (MBE)^[2,3] and Metalorganic Chemical Vapor Deposition MOCVD growth^[4,5]. Optimized structures exhibit reduced threshold current density and lower temperature sensitivity as compared to conventional InP-based 1.3 μm emitting lasers. One challenging goal remaining is to extend the emission wavelength beyond 1.3 μm , while maintaining optical material quality for the realization of longer wavelength, high-performance, GaAs based devices. Wang et al. found that adding antimony as a surfactant during GaInNAs growth allowed longer wavelength devices^[6]. From $k \cdot p$ methods, it was theoretically predicted that nitride-antimonide alloys should possess similar bowing to the nitride-arsenide^[7]. This was experimentally validated when it was found that cracked antimony incorporates into the crystal^[8,9], further redshifting emission and allowing the demonstration of lasers operating in pulsed mode out to 1.49 μm ^[10]. In this work, we used an experimental technique, the photocurrent (PC) together with photoluminescence (PL) techniques to investigate the

electronic and optical properties of GaInNAs/GaAs quantum well and compared the results with those obtained from a sequentially grown GaInNAsSb/GaAsSbN quantum well.

MATERIALS AND METHODS

In this study, two quantum wells (QWs) were grown by molecular beam epitaxy on an n-type GaAs (100) substrate using a radio frequency (rf) N radical beam source. The active region consists of 7 nm GaIn_{0.37}N_{0.013}As or GaIn_{0.4}N_{0.01}AsSb_{0.015} quantum wells sandwiched between 100 nm undoped GaAs waveguide layers. The GaInNAsSb single QW is surrounded by GaN_{0.01}AsSb_{0.015} barriers. A 1.5 μm Si-doped (7×10^{17}) n-type Al_{0.8}Ga_{0.2}As cladding layers was grown between the n+-GaAs buffer layer (0.2 μm) and the active layer. A 1.5 μm Be-doped (5×10^{17}) p-type Al_{0.8}Ga_{0.2}As cladding layers followed the active layer. Conventional InZn metallization was used for the p-type contact. The growth temperature for the QWs, the GaAs waveguide layer and AlGaAs cladding layer were 400, 510, 550°C, respectively. To determine the N and In mole fractions, both X-ray diffraction and pre-calibrated PL investigations of InGaAs structures were performed.

The PC spectra were performed using a halogen lamp dispersed by a 0.25-m Jobin-Yvon monochromator. The chopped monochromatic light was incident on the top of the sample and the capacitively

coupled photoresponse signal was obtained by measuring the open circuit voltage (V_{oc}) using the lock-in amplifier. The PL measurements were carried out using a variable temperature (10-300K) close-cycle cryostat under the excitation of 514.5 nm line of an Argon ion Ar^+ laser. The signal was detected through a 0.25-m Jobin-Yvon monochromator and by a GaInAs photodiode associated with a standard lock-in technique.

RESULTS AND DISCUSSION

Room temperature photocurrent spectra of GaInNAs and GaInNAsSb QWs are shown in Fig. 1. We note that photocurrent spectra of the two samples are formed by well-defined absorption steps and the incorporation of Sb red shifts the fundamental gap to 850 meV. The arrows show the calculated transitions using the nominal thickness, as discussed below. The confined energies of the electrons, heavy and light holes are calculated using the envelope function formalism. The unstrained band gap energy E_g^{ust} of III(Ga,In)-V(As,Sb)-N layer is determined using the Band Anticrossing Model (BAC)^[11] and the strained band gap energy E_{e-hh}^{st} (III-V-N) between the electron and the heavy (light) hole bands is determined taking into account the hydrostatic and shear components of the strain, given by:

$$E_{e-hh}^{st}(\text{III-V-N}) = E_g^{ust}(\text{III-V-N}) + E_{hyd} + E_{sh} \quad (1)$$

$$E_{e-hh}^{st}(\text{III-V-N}) = E_{e-hh}^{st}(\text{III-V-N}) - 1.5E_{sh} + 0.5\Delta_{so} \left[1 - \sqrt{1 + 2E_{sh}/\Delta_{so} + 9E_{sh}^2/\Delta_{so}^2} \right] \quad (2)$$

$$E_{hyd} = \left[2(p + \Delta p)(C_{11} - C_{12})/C_{11} \right] \epsilon; \\ E_{sh} = \left[-q(C_{11} + 2C_{12})/C_{11} \right] \epsilon \quad (3)$$

Where, p and q are respectively the hydrostatic and shear deformation potentials and C_{ij} the elastic constants in (In,Ga)As system. Δ_{so} is the spin-orbit splitting which is independent of nitrogen content^[12]. Δp is the shear deformation potential term correction due to N and Sb in III-V materials. ϵ is relative strain in the plane direction. The electron effective mass in the III-V-N layer is taken as:

$$m_e(\text{III-V-N}) = m_e(\text{III-V}) + \Delta m_e \quad (4)$$

Where, $m_e(\text{III-V})$ is the electron effective mass in III-V material and Δm_e is the electron effective mass term correction resulting from the flattening of the conduction band under nitrogen effect. The strained conduction band offset used in our calculation is about

80% of the strained heavy hole-electron bandgap difference; this value is the same as for GaInNAs/GaAs QWs with comparable indium and nitrogen contents^[13]. Figure 2 shows GaInNAs/GaAs QWs calculated transitions energies plotted as a function of the electron effective mass correction for different Δp shear terms correction. Observed transitions energies are indicated as dark squares. A reasonable agreement is found for the E_1-H_1 , E_1-L_1 and E_2-H_2 data using $\Delta p/p=0.11$ and $\Delta m_e=0.035 m_0$. The E_1-H_1 and E_1-L_1 measured transitions of GaInNAs(Sb)/GaAsSbN SQW are in agreement with the theoretical fit for $\Delta p/p=0.3$ and $\Delta m_e=0.035 m_0$. We have plotted in Fig. 3 the band-edge profiles of GaInNAs/GaAs and GaInNAs(Sb)/GaAsSbN QWs showing the type I band alignment. We note that the incorporation of Sb in GaInNAsSb/GaAsSbN have reduced the fundamental gap energy and the electron potential depth from 418 meV to 340 meV by comparison with GaInNAs/GaAs QWs.

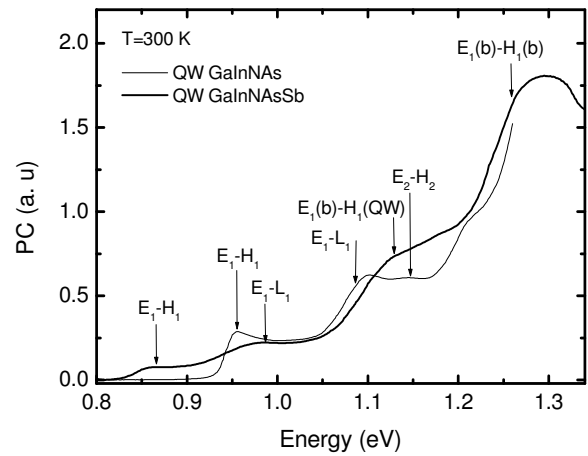


Fig. 1: Room temperature photocurrent spectra of GaInNAs and GaInNAsSb quantum wells

PL spectra of GaInNAs and GaInNAsSb QWs are shown, respectively, in Fig. 4a and b at different temperatures. We note that from 300 to 10 K, the PL peak energy increases from 0.935 to 0.977 eV for GaInNAs and from 0.866 to 0.913 eV for GaInNAsSb QWs. The redshift shift ΔE between 10 K and 300 K is noticeably lower for GaInNAsSb QW (47 meV) than for GaInNAs QW (61 meV). To clarify this point, we have reported in Fig. 5 the temperature dependence of the PL peak energy. The E_1-H_1 energy dependence with temperature measured by PC in the two samples is also shown. The dashed lines are the fits using Bose Einstein model^[14]:

$$E_g(T) = E_B - a \left[\frac{2}{\exp(\theta/T) - 1} + 1 \right] + \alpha K_B T \quad (5)$$

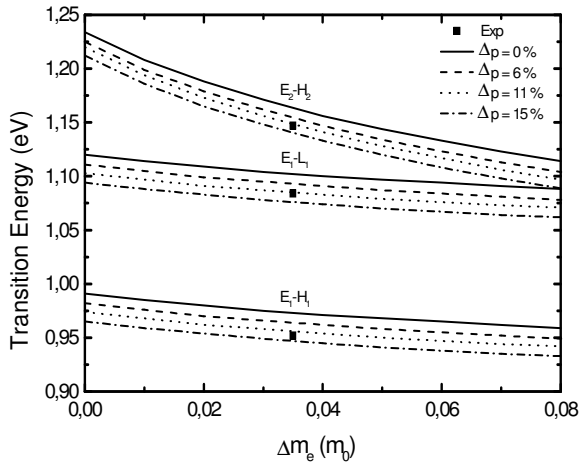


Fig. 2: Room temperature transition energies of GaInNAs as function of the electron effective mass term correction with the theoretical fit (solid and dashed lines) for different Δp shear deformation potential term correction

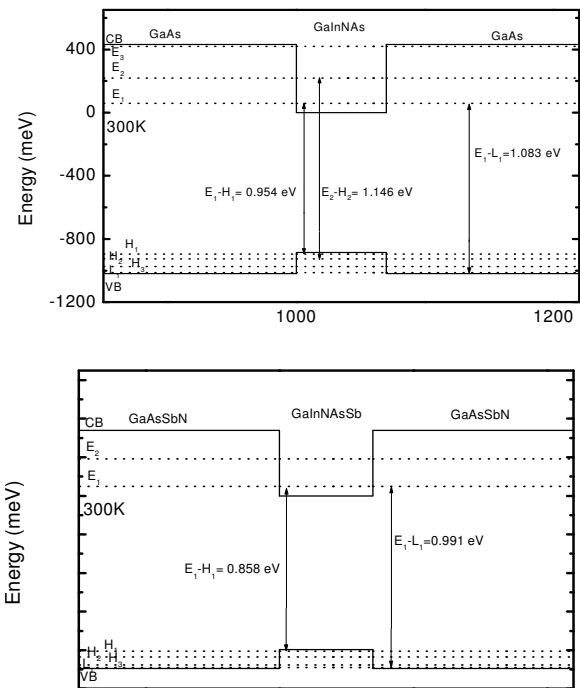


Fig. 3: Room temperature band-edge profiles for GaInNAs and GaInNAsSb quantum wells

Where, $(E_B - a)$ is the transition energy at 0 K, a is the electron phonon interaction strength and θ is related to the average phonon energy. α is the parameter reflecting the shape of the density of states which is assumed to be about 0.5 here and K_B is the Boltzmann constant. It is shown that the temperature dependence of PC peak energy can be fitted well by equation (5). For GaInNAs and GaInNAsSb QWs, the optimum fit parameters a and θ are, respectively equal to 128, 97 meV and 410, 340 K. We note that both the electron-

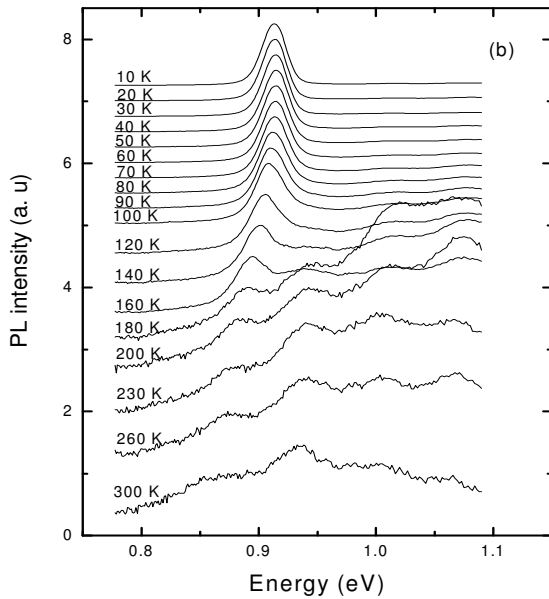
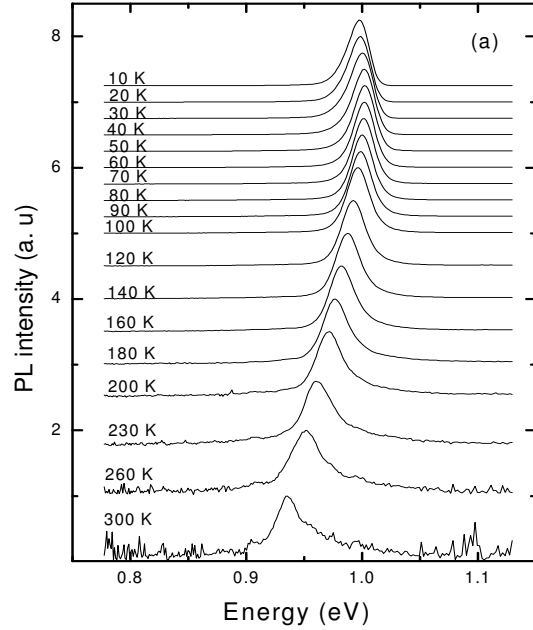


Fig. 4: (a) PL spectra of GaInNAs and (b) GaInNAsSb quantum wells at various temperatures

phonon interaction strength and the average phonon energy decrease with decreasing the nitrogen content from 1.3 % in GaInNAs to 1% in GaInNAsSb QWs. We have noted that the measured electron-phonon interaction strengths are in agreement with that given by H. Yaguchi *et al.*^[15] in GaAsN layers with comparable nitrogen compositions. In addition, the evolution of the PL peak energy of GaInNAs QW (closed circles) as function of temperature is the same as that of the E_1-H_1 transition (open circles), except at low temperature (10 K) when the PL peak energy is situated at about 13 meV below the E_1-H_1 energy. In contrast, the temperature dependence of the PL peak

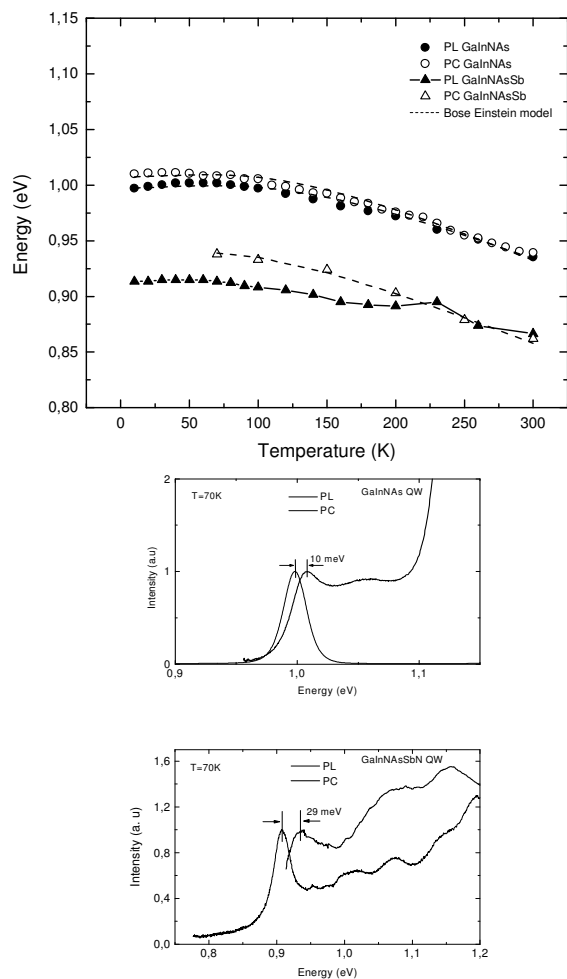


Fig. 5: PL temperature dependence of the emission peak of the GaInNAs (closed circles) and of the GaInNAsSb (closed triangles) QWs. Solid line is a guide to the eyes. Open circles and open triangles represent the E_1-H_1 energies of the GaInNAs and GaInNAsSb QWs respectively. The dashed line is a Bose Einstein fit to the PL and PC measurements of the two QWs. The PC and PL Spectra of the two QWs at 70K are shown in the inset

energy of GaInNAsSb QW have an anomalous behaviour, the so-called inverted S shape behavior indicating a transition between recombination from localized and delocalized states. The anomalous temperature induced shift of the emission energy has already been observed by other groups in N containing III-V alloys^[16-19] and it was attributed to localized exciton emission. Between 8 and 160 K a redshift appears and is believed to be a result of exciton trapping into lower energy localized states. In this region the excitons acquire thermal energy as the temperature increases allowing them to overcome small potential barriers and fall into the lower lying states. However, when the temperature reaches 160 K,

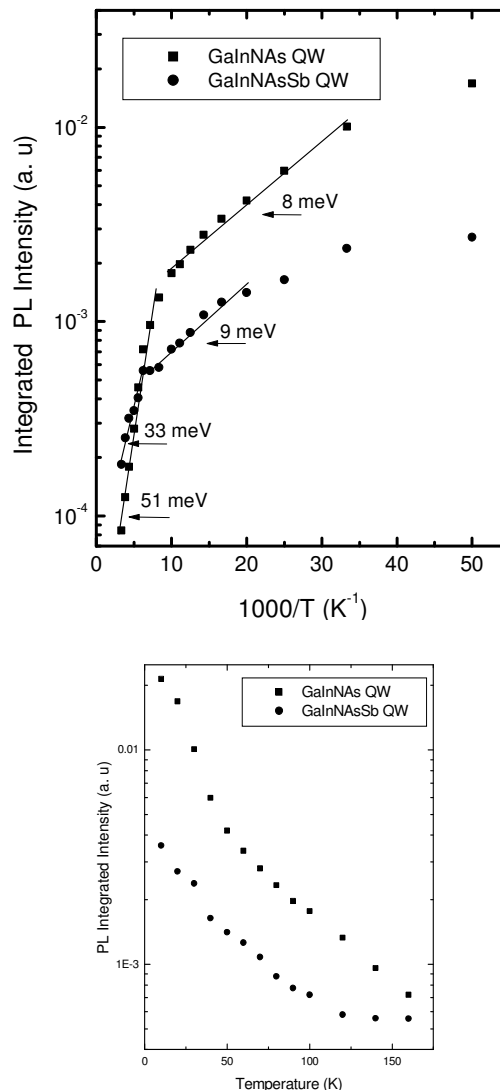


Fig. 6: Integrated PL intensity (log scale) plotted as a function of reciprocal temperature for GaInNAs (closed square) and GaInNAsSb (closed circle) quantum wells

excitons in shallow localized states acquire sufficient thermal energy to become delocalized. As more and more excitons become delocalized, the resulting emission is blue-shifted until the system become fully delocalized at the delocalized temperature about 230 K. Finally excitons are completely delocalized and the PL peak energy is mainly determined by the behaviour of the bandgap as verified by PC measurements. This S-shape explains why the shift between 10 and 300 K, which is directly seen in Fig. 4, is lower for GaInNAsSb QW than for GaInNAs. We show in the inset of Fig. 5 the PC and PL Spectra of the two QWs at 70K. The strong energy shift between E_1-H_1 and the PL peak for GaInNAsSb (29 meV) compared to that of GaInNAs QW (10 meV) shows a high density of possibly deep localizing potential wells. This can be

explained probably by the fact that when Sb atoms are incorporated into GaInNAs, the density of N clusters and the related potential fluctuation are increased due to the diminution of the preferable formation of N-In covalent bonds. In fact, In-N bonds help N clusters to segregate from lattice and reduce the azote induced potential fluctuations^[20].

Temperature dependence of PC is shown in the inset of Fig. 6. The PL intensity of GaInNAs and GaInNAsSb QWs decreases rapidly with increasing temperature. In order to analyse temperature dependence of PL, we plotted the logarithm of the integrated PL intensity as function of reciprocal temperature as shown in Fig. 6. The samples show a remarkable behavior characterized by two temperature regimes both of which obey an Arrhenius relationship. The low temperature activation energy E_{a1} derived by the linear part of the plot, was found to be 9 meV and 8 meV respectively for GaInNAsSb and GaInNAs QWs; and the high temperature activation energy E_{a2} was found to be 33 meV and 51 meV respectively for GaInNAsSb and GaInNAs QWs. Like other works, the activation energies increase with the azote incorporation^[21,22]. For an alternative explanation, E_{a1} is related to the ionization of impurity bound excitons. On the other hand, the deep traps are the most likely cause of the thermal activation energy E_{a2} .

CONCLUSION

Optical properties of GaInNAs and GaInNAsSb QWs have been investigated by photocurrent and photoluminescence spectroscopy. In the case of PC measurements, we have observed optical transitions in the two samples. Based on calculations from experimental data, we have found an increase of the electron effective mass by as much as $0.035 m_0$ and the conduction band offset is about 80 %. Moreover, we find less temperature dependence of the PL energy of the sample containing antimony due to the deeper localized states. This behaviour can be explained probably by the fact that when Sb atoms are incorporated into GaInNAs, the density of N clusters and the related potential fluctuation are increased due to the diminution of the preferable formation of N-In covalent bonds

REFERENCES

1. Kondow, M., K. Uomi, A. Niwa, T. Kitatani, S. Watahiki and Y. Yazawa, 1996. *Jpn. J. Appl. Phys.*, 33: 1273.
2. Livshits, D.A., A.Y. Egorov and H. Riechert, 2000. *Electron. Lett.*, 36: 1381.

3. Fisher, M., D. Gollub, M. Reinhardt, M. Kamp and A. Forchel, 2003. *J. Crystal Growth*, 251: 353.
4. Takeuchi, T., Y.L. Chang, M. Leary, A. Tandon, H.C. Luan, D. Bour, S. Corzine, R. Twist and M. Tan, 2002. *Electron. Lett.*, 38: 1438.
5. Kawaguchi, M., T. Miyamoto, E. Gouardes, D. Schlenker, T. Kondo, F. Koyama and K. Iga, 2001. *Jpn. J. Appl. Phys. 2-Lett.*, 40: L744.
6. Yang, X., M.J. Jurkovic, J.B. Heroux and W.I. Wang, 1999. *Appl. Phys. Lett.*, 75: 178.
7. Murdin, B.N., A.R. Adams, P. Murzyn, C.R. Pidgeon, I.V. Bradley, J.P.R. Wells, Y.H. Matsuda, N. Miura, T. Burke and A.D. Johnson, 2002. *Appl. Phys. Lett.*, 81: 256-258.
8. Shimizu, H., K. Kumada, S. Uchiyama and A. Kasukawa, 2000. *Electron. Lett.*, 36: 1701-1703.
9. Gambin, V., W. Ha, M. Wistey, H. Yuen, S.R. Bank, S.M. Kim, J.S. Harris Jr., 2002. *IEEE J. Select. Topics Quantum Electron*, 8: 795-800.
10. Ha, W., V. Gambin, S. Bank, M. Wistey, H. Yuen, S. Kim and J.S. Harris Jr., 2002. *IEEE J. Quantum Electron*, 38: 1260-1267.
11. Shan, W., W. Walukiewicz, J.W. Ager III, E.E. Haller, J.F. Geisz, D.J. Friedman, J.M. Olson, S.R. Kurtz, 1999. *Phys. Rev. Lett.*, 82: 1221-1224.
12. Perkins, J.D., A. Mascarenhas, Y. Zhang, J.F. Geisz, D.J. Friedman, J.M. Olson, S.R. Kurtz, 1999. *Phys. Rev. Lett.*, 82: 3312-3315.
13. Hetterich, M., M.D. Dawson, A. Yu. Egorov, D. Bernklau and H. Riechert, 2000. *Appl. Phys. Lett.*, 76: 1030-1032.
14. Lautenschlager, P., M. Garriga, S. Logothetidis and M. Cardonna, 1987. *Phys. Rev. B.*, 35: 9174.
15. Yaguchi, H., S. Kikuchi, Y. Hijikata, S. Yoshida, D. Aoki and K. Onabe, 2001. *Phys. Stat. Sol.(b)*, 228: 273-277.
16. Grenouillet, L., C. Bru. Chavalier, G. Guillot, P. Gilet, P. Duvaut, C. Vannuffel, A. Million and A. Chenevas-Paule, 2000. *Appl. Phys. Lett.*, 76: 2241.
17. Pinault, M.A. and E. Tournié, 2001. *Appl. Phys. Lett.*, 78: 1562.
18. Cho, Y.H., G.H. Gainer, A.J. Fischer, J.J. Song, S. Keller, U. K. Mishra, *et al.*, 1998. *Appl. Phys. Lett.*, 73: 1370.
19. Hoffmann, A., R. Heitz, A. Kaschner, T. Luttgert, H. Born, A.Y. Egorov and H. Riechert, 2002. *Mater. Sci. Engg. B.*, 93: 55-59.
20. Sun, B.Q., D.S. Jiang, Z. Pan, L.H. Li and R.H. Wu, 2000. *Appl. Phys. Lett.*, 77 : 4148.
21. Zhou, W., S.J. Chua, J.R. Dong and J.H. Teng, 2002. *J. Cryst. Growth.*, 242 : 15-19.
22. Sanorpim, S., F. Nakajima, R. Katayama, K. Onabe and Y. Shiraki, 2003. *Mat. Res. Soc. Symp. Proc.*, 744 : M10.9.1.